# Clinical and Pathologic Features of Oligodendrogliomas in Two Cats

P. J. Dickinson, M. K. Keel, R. J. Higgins, P. D. Koblik, R. A. Lecouteur, D. K. Naydan, A. W. Bollen and W. Vernau

*Vet Pathol* 2000 37: 160
DOI: 10.1354/vp.37-2-160

Vet Pathol **37**:160–167 (2000)

# Clinical and Pathologic Features of Oligodendrogliomas in Two Cats

P. J. DICKINSON, M. K. KEEL, R. J. HIGGINS, P. D. KOBLIK, R. A. LECOUTEUR, D. K. NAYDAN, A. W. BOLLEN, W. VERNAU

Departments of Surgery and Radiology (PJD, PDK, RAL) and Pathology, Microbiology and Immunology (MKK, RJH, DKN, WV), School of Veterinary Medicine, University of California, Davis, CA; and
Department of Pathology, School of Medicine, University of California, San Francisco, CA (AWB)

**Abstract.** Two oligodendrogliomas in two domestic cats involved mainly the rostral brain stem, midbrain, fourth ventricle, and cerebellum. Both cats were aged neutered males presenting with clinical neurologic deficits suggestive of a brain stem lesion. Magnetic resonance imaging of both tumors demonstrated lesions with a pattern of heterogeneous contrast enhancement and multifocal lesions in one cat. Routine cerebrospinal fluid analysis was normal in one cat and suggestive of an inflammatory disease in the other. Oligodendroglioma cells were seen in cytospin preparations of cerebrospinal fluid from both cats. In each cat, the tumors occurred intraventricularly in the midbrain and fourth ventricle with aggressive intraparenchymal infiltration. There was extensive growth into the basilar subarachnoid space of the midbrain and brain stem in one cat. One tumor was well differentiated, and the other was an anaplastic subtype. Immunostaining for several myelin- and oligodendroglia-specific antigens was negative with formalin-fixed tumors and with unfixed frozen samples from one cat. In both tumors, component cells of the intratumoral vascular proliferations were positive for human von Willebrand factor VIII antigen or smooth muscle actin. Immunocytochemical reactivity for glial fibrillary acidic protein identified both reactive astrocytes and a subpopulation of minigemistocytes in both tumors. Ultrastructurally, the tumor cells were unremarkable except for their prominent desmosomal junctions and paucity of microtubules.

*Key words:* Cats; cerebellum; cerebrospinal fluid; immunocytochemistry; magnetic resonance imaging; oligodendroglioma; ultrastructure.

In the domestic cat, spontaneous tumors of the central nervous system (CNS) are relatively rare; the most common are meningiomas and multicentric lymphoma.[8,23] Feline oligodendrogliomas have been rarely described and then only in the brain.[6,12,17,19] There is only one case with a description of the clinical findings and microscopic pathology.[18] Two presumptive feline oligoastrocytomas have been reported.[3,4] Here, we report two feline cases of oligodendroglioma with results of magnetic resonance imaging (MRI), neurologic examination, cerebrospinal fluid (CSF) analysis, detailed microscopic and ultrastructural evaluation, and immunocytochemical staining for some marker antigens of oligodendroglia and myelin.

## Materials and Methods

### Cats

Cat No. 1 was a-year-old castrated male domestic shorthair that was presented to the Veterinary Medicine Teaching Hospital (VMTH) at the University of California–Davis (UC Davis) for investigation of recumbency and apparent pain of vague origin. Inability to walk had been progressive over a 5–6-week period. The animal was an indoor/outdoor cat and was fully vaccinated, with no travel history. A recent feline leukemia virus antigen serologic test was negative.

Cat No. 2 was an 11-year-old castrated male domestic shorthair that was presented to VMTH, UC Davis, with a history of compulsive pacing of 1 month duration and more recent obtundation and ataxia of 9 days duration. Empirical treatment with dexamethasone and amitriptyline for 7 days prior to presentation had not altered the progression of clinical signs. The animal was an indoor cat and was fully vaccinated, with no travel history.

### Neuroimaging

Under general anesthesia, MRI of the heads of both cats was performed using a 0.4 Tesla scanner (Resonex 5000, Resonex, Sunnyvale, CA). Contiguous 4-mm transverse images were generated with T1 weighted, T2 weighted, and proton weighted (PW) spin echo pulse sequences. Contiguous 4-mm sagittal images were generated with PW spin echo pulse sequences. Additional T1 weighted transverse and sagittal images were acquired after administration of intravenous contrast medium at 0.2 ml/kg (Magnevist, 100 mg/ml gadopentatate dimeglumine, Berlex Labs, Wayne, NJ).

### Pathologic examination

Following euthanasia, both cats were submitted for complete necropsy. Brains and representative samples of other

tissues were immersed in 10% buffered formal saline, and 1 week later the brains were sectioned transversely at 3-mm intervals. These and other tissue sections were routinely processed, embedded in paraffin, cut at 5 μm, stained with hematoxylin and eosin (HE), and examined with a microscope. A fresh tissue sample from the tumor of cat No. 2 was immediately frozen in Tissue-tek O.C.T. compound (Sakura Finetek USA, Torrance, CA) using methyl butane cooled with liquid nitrogen and then was stored at −90 C prior to immunocytochemical staining. Some selected sections were also stained with Masson's trichrome, Alcian blue, mucicarmine, and Von Kossa's stains.

### Immunocytochemical staining

Sections of paraffin-embedded tumor tissue from both cats and fresh frozen tumor from cat No. 2 were stained immunocytochemically using a labeled streptavidin–biotin method as previously described, with the following modifications.[15] Prior to staining, frozen sections were fixed in cold acetone (−10 C) for 10 minutes. All sections were pretreated with an avidin–biotin blocking procedure (blocking kit SP-2001, Vector Laboratories, Burlingame, CA). Primary antibodies used were mouse monoclonal antibodies to cultured murine and canine oligodendrocytes (ascitic fluid dilution 1 : 10, Professor M. Vandevelde, University of Berne, Berne, Switzerland), to the canine common leucocyte antigen CD45R (1 : 10, Dr. P. F. Moore, UC Davis, Davis, CA), to galactocerebroside (1 : 20, Boehringer Mannheim, Indianapolis, IN), to synaptophysin (1 : 100, Boehringer Mannheim), to CD57/HNK-leu7 (1 : 100, Biocare Medical, Walnut Creek, CA), to alpha smooth muscle actin (1 : 100, Biogenex Laboratories, San Ramon, CA), to triple (pan) neurofilament protein (1 : 100, Zymed Laboratories, South San Francisco, CA), and to MIB-1 (1 : 80, Oncogene Research Products, Cambridge, MA) and rabbit polyclonal antibodies (Dako Corp., Carpinteria, CA) to human Von Willebrand factor VIII (1 : 2,000), bovine glial fibrillary acidic protein (GFAP) (1 : 1,200) and human myelin basic protein (MBP) (1 : 300). Negative controls were prepared by omitting the primary antibody and substituting a mouse myeloma isotype correlate or an irrelevant rabbit IgG antibody. Immunostaining using our appropriate standard positive control tissue for each of these antibodies was done in parallel.

### Electron microscopy

Selected samples of tumor tissue from cat No. 2 that were originally fixed in 10% formalin were postfixed for 24 hours in 2% glutaraldehyde in 0.1 M cacodylate buffer, pH 7.4. After routine processing, plastic-embedded thick sections were stained with toluidine blue, and thin sections were cut from selected areas, stained, and then examined ultrastructurally with a Zeiss 10 transmission electron microscope as previously described.[9]

## Results

### Clinical findings

*Cat No. 1.* Physical examination revealed obesity, mild bilateral conjunctivitis with serous discharge, mild crusting around the nares bilaterally, and marked dental tartar with mild gingivitis. The cat resented handling, particularly palpation of the spinal column. Neurologic examination revealed a mildly obtunded mentation with nonambulatory tetraparesis, positional nystagmus, and opisthotonus when placed in dorsal recumbency. A diagnosis of central vestibular disease was made based on the results of the neurologic examination. Thoracic radiographs, abdominal ultrasound, serum chemistry (including creatine kinase), complete blood count (CBC), and urinalysis were unremarkable other than a mild lymphopenia (882 cells/μl). MRI demonstrated a large heterogeneously contrast-enhancing mass in the area of the rostral cerebellum and fourth ventricle, with dilation of the lateral and third ventricles. The mass was poorly marginated and predominantly hyperintense on PW and T2 weighted images. There was soft tissue opacification of both compartments of the right bulla and of the ventral compartment of the left bulla. Contrast enhancement was seen involving the periphery of these areas. There was no bacterial growth from fluid obtained at myringotomy. No apparent continuity was present between the mass lesion and the bullae. The animal was euthanatized 6 weeks after initial presentation because of progression of clinical signs.

*Cat No. 2.* Physical examination revealed moderate dehydration and bilaterally luxating patellas. Increased jaw tone prevented manual opening of the jaws. On neurologic examination, the animal was slightly obtunded but responsive. Abnormal mentation was suggested by constant staring into space. The animal was weakly ambulatory with support with marked truncal ataxia and hypermetria. Extensor tone was increased in the pelvic limbs. The menace response was decreased in the left eye; however, vision was present bilaterally with intact visual tracking. Conscious proprioception and hopping were depressed in all four limbs; the right thoracic limb was least affected. Segmental spinal reflexes were within normal limits. Apparent pain was present with extension of the neck and palpation of the mid thoracic spine. A diagnosis of intracranial disease with involvement of the brain stem was made based on clinical signs. Thoracic radiographs, abdominal ultrasound, serum chemistry, CBC, and urinalysis revealed a mild lymphopenia (616 cells/μl) and mild thrombocytopenia (172,000 cells/μl). MRI demonstrated two separate masses, both of which were hyperintense on T2-weighted and PW images and hypointense on T1-weighted images and had strong heterogeneous contrast enhancement. The first lesion was present along the ventral aspect of the brain stem, predominantly left sided, from the level of the caudal aspect of the cerebellum to the midbrain with right and dorsal displacement of the brain stem (Fig. 1). The second lesion was in the fourth ventricle be-

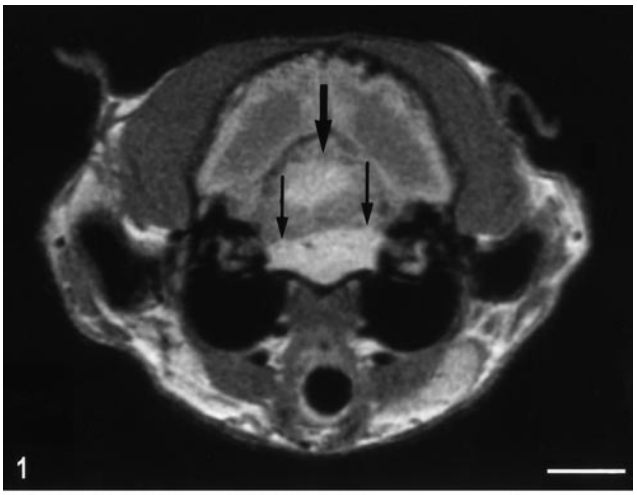


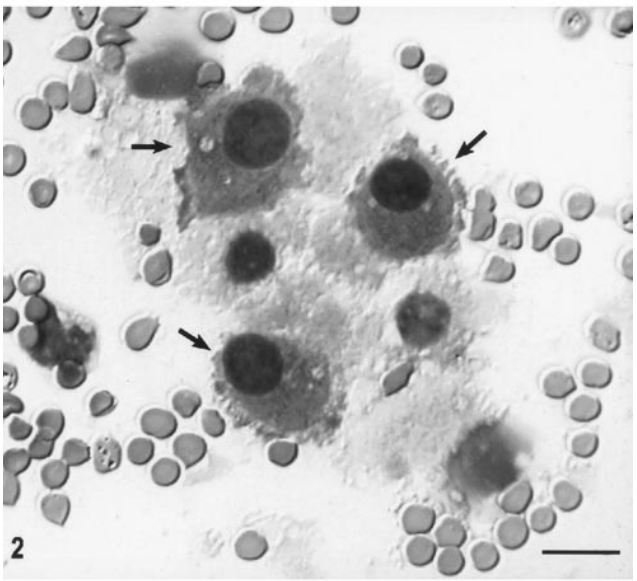


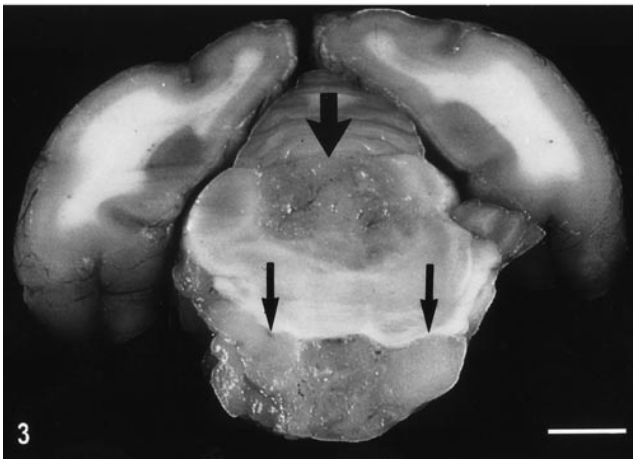


**Fig. 1.** Head; cat No. 2. MRI section at the level of the cerebellum and fourth ventricle; T1-weighted image. Note the separate contrast-enhancing masses within the fourth ventricle (wide arrow) and in the basilar meninges (thin arrows). Bar = 1 cm.

**Fig. 2.** CSF cytospin preparation, cat No. 1. Note the large presumptive tumor cells with large, round, dense slightly eccentric nuclei and densely staining bluish cytoplasm with ruffled cytoplasmic borders (arrow). Other cells are macrophages. Wright's stain. Bar = 16 μm.

**Fig. 3.** Fixed brain; cat No. 2. Compare this transverse section to that in Fig. 1, with the intraventricular localization of the oligodendroglioma (wide arrow) and prominent growth in the basilar meninges (thin arrows). Bar = 33 mm.

tween the cerebellum and the midbrain. Rostral to the masses, there was marked hydrocephalus involving the lateral and third ventricles. Because of the poor neurologic status and prognosis, the owners elected euthanasia.

### Clinical pathology

*Cat No. 1.* CSF analysis indicated a normal protein level (21 mg/dl), a total red blood cell count (RBC) of 144 cells/μl, and a normal nucleated cell count (2 cells/μl) with a differential white cell count of 15% neutrophils, 31% small mononuclear cells, 53% large mononuclear cells, and 1% eosinophils. There were some large tumor cells with a uniformly round nucleus and abundant deeply basophilic cytoplasm whose borders often formed globular projections (Fig. 2). These cells were often paired or sometimes in aggregates. Occasional mitotic figures were noted.

*Cat No. 2.* CSF analysis indicated an elevated protein content (189 mg/dl), a total RBC of 138 cells/μl, and an elevated total nucleated cell count of 33 cells/μl with a differential count of 7% neutrophils, 67% small mononuclear cells, and 26% large mononuclear cells. Tumor cells morphologically similar to those in cat No. 1 were noted. Impression smears of the tumor that were stained with Wright's stain had aggregations of very uniform cells with a round nucleus and thin rim of cytoplasm associated with prominent hyperplastic capillaries.

### Gross necropsy findings

*Cat No. 1.* On external examination of the brain, there was only a slight dorsal swelling and protrusion of the cerebellar vermis. On transverse sections, these changes were due to a single, well demarcated, round mass in the fourth ventricle and extending within and distending the mesencephalic aqueduct rostrally to the level of the rostral colliculus. Although most of the mass was intraventricularly located, there was extension to the surface at the level of the rostral colliculus. The mass measured up to 1.2 cm diameter in the fourth ventricle and on cut surface had a gelatinous translucent appearance, with small scattered red foci. Rostral to the mass, the third and both lateral ventricles were moderately enlarged. The cat also had a unilateral suppurative otitis media.

*Cat No. 2.* On the ventral aspect of the brain, there was a pearlescent, white to tan colored, well demarcated, firm, almost symmetrical mass extending caudally about 3.5 cm from the optic chiasm. The greatest thickness and width (1.5 × 0.5 cm) was on the left side at the level of the hypoglossal nerve. On the transverse sections, this mass partially compressed the overlying brain stem and midbrain (Fig. 3). Grossly, there was an apparently separate second mass (0.8 × 0.6 cm) of similar appearance and texture within and distending the lumen of the fourth ventricle (Fig. 3). No other lesions were found.

**Microscopic findings**

*Cat No. 1.* The microscopic appearance of this anaplastic oligodendroglioma was similar in all transverse sections examined. The tumor was composed of diffuse sheets of cells with a thin border zone of infiltration into the adjacent parenchyma. Tumor cells had usually round to slightly ovoid, hyperchromatic nuclei of various sizes, with prominent single nucleoli and a variable amount of eccentrically distributed eosinophilic cytoplasm. Tumor cells also had a very prominent cytoplasmic membrane. There were up to four mitotic figures per 40X high-power field (HPF). There were multiple foci of necrosis, and these foci often contained areas of extensive calcification (Fig. 4). Within the solid areas of the tumor, there were also interstitial accumulations of a mucopolysaccharide-like substance that sometimes coalesced into cysts of various sizes and that stained positively with Alcian blue and mucicarmine. A feature of the tumor in some areas was the formation of clusters or long lines of prominent blood vessels forming glomeruloid structures (Fig. 5a). There was tumor extension under the subpial membrane superficially in the brain and also partial obliteration by the tumor of the ependymal lining of the mesencephalic aqueduct and fourth ventricle.

*Cat No. 2.* This well-differentiated oligodendroglioma had cytologic features similar to those of the tumor in cat No. 1, but the major differences were the lack of intratumoral necrosis and calcification, the cell cytoplasm was less prominent and had less intense eosinophilic staining, and the nuclei were more uniform and round. There was up to one mitotic figure per 40X HPF. Intratumoral lakes or cysts containing mucopolysaccharide-like material tended to be much larger. There was strikingly extensive tumor growth within the subarachnoid space with entrapment of, but no morphologic changes in, many cranial nerve roots in the brain stem area (Fig. 6). There were residual segments of ependyma partially lining the fourth ventricle. Examination of sequential transverse segments indicated that the tumor foci within the ventricular sys-

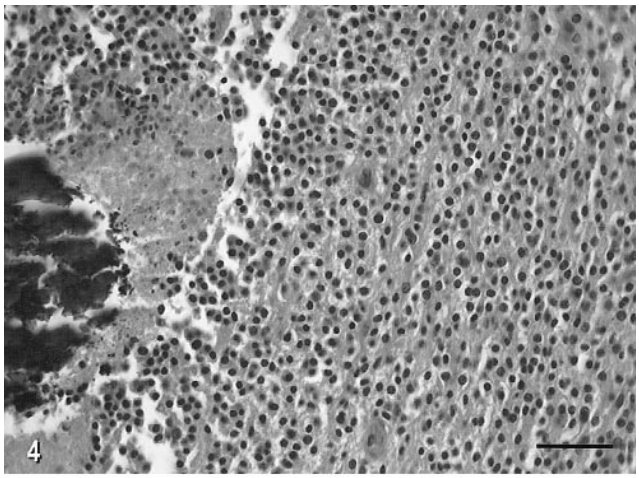


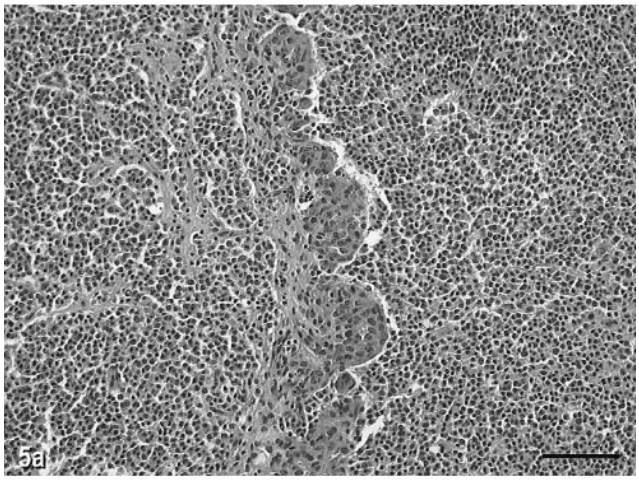


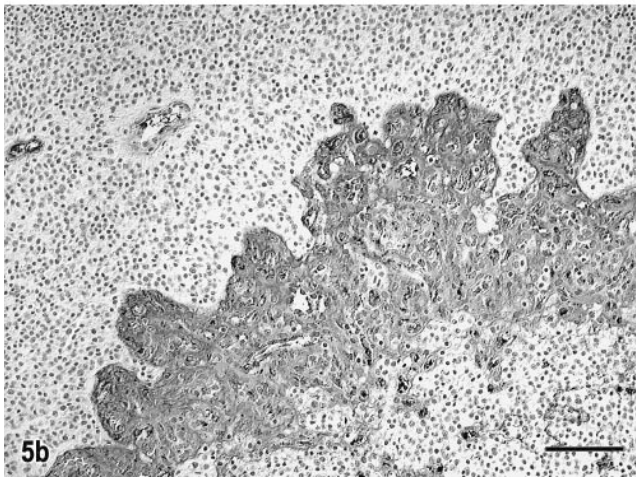


**Fig. 4.** Anaplastic oligodendroglioma, brain; cat No. 1. There are several foci of acute necrosis with central mineralization. Note the sheets of round to ovoid nuclei with prominent eosinophilic cytoplasm. HE. Bar = 70 μm.

**Fig. 5.** Anaplastic oligodendroglioma, brain; cat No. 1. **Fig. 5a.** Note the line of prominent glomeruloid vascular proliferation. HE. Bar = 80 μm. **Fig. 5b.** Immunocytochemical localization of human von Willebrand factor VIII antigen in the glomeruloid vascular proliferation in cat No. 1. Streptavidin–biotin stain. Bar = 50 μm.

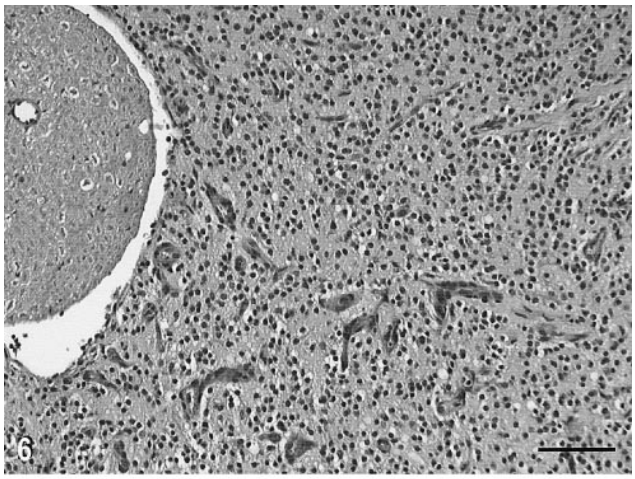


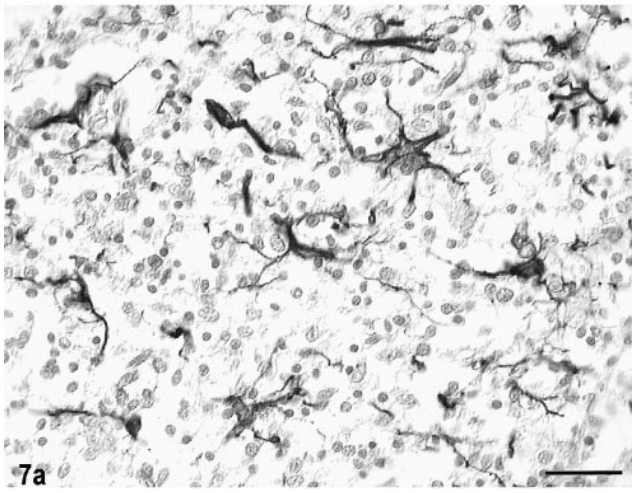


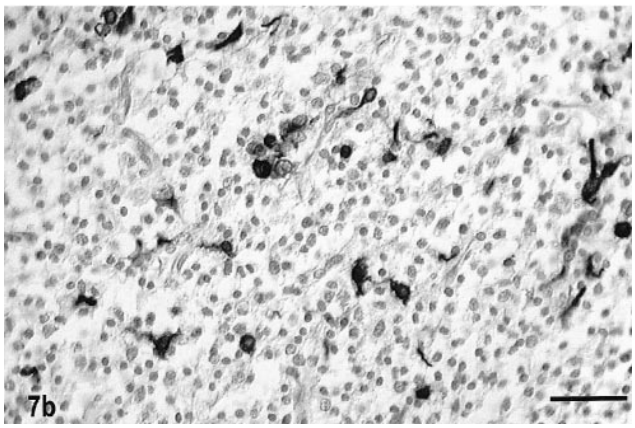


**Fig. 6.** Oligodendroglioma, brain; cat No. 2. Extension of the tumor into the basilar subarachnoid space. Note the entrapment of the nerve root, which is morphologically intact. HE. Bar = 60 μm.

**Fig. 7.** Oligodendroglioma, brain, cat No. 2. **Fig. 7a.** Numerous reactive astrocytes are present throughout the tumor. Streptavidin–biotin for GFAP. Bar = 40 μm. **Fig. 7b.** Numerous GFAP-positive, GFOC-like cells. Note the cytoplasmic staining pattern with the thin round rim of perinuclear localization of GFAP and with minimal processes. Streptavidin biotin for GFAP. Bar = 40 μm.

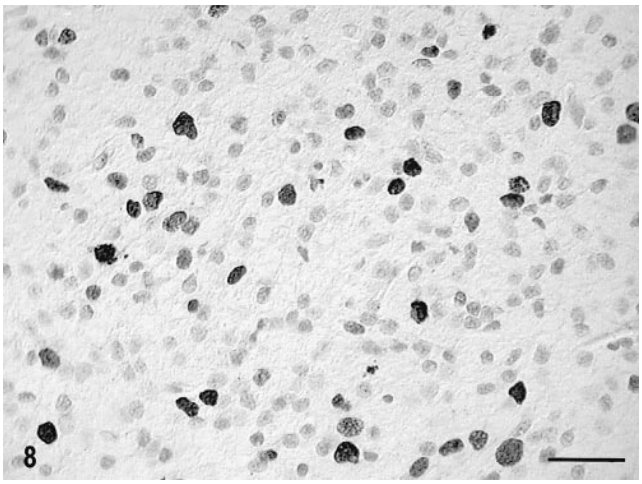


**Fig. 8.** Tumor cell nuclei, brain; cat No. 1. MIB-1 positivity. Streptavidin–biotin for MIB-1. Bar = 34 μm.

tem, subarachnoid space, and parenchyma were all confluent. Microscopic tumor foci isolated from the main mass were detected in the subarachnoid space of the cerebellum. There was also local tumor infiltration within the meninges.

### Immunocytochemistry

In both cats, there was prominent staining for human von Willebrand factor VIII antigen in the tumor blood vessels, particularly in the clusters and loops of hypertrophy and hyperplasia (Fig. 5b); these vessels also contained some cells staining positively for smooth muscle actin. There were marked regional differences in the density of capillaries in different areas of the tumors. In cat No. 1, there were few cells staining positively with GFAP. In most areas of tumor in cat No. 2, about 3% of the GFAP-positive cells most resembled reactive astrocytes in morphology (Fig. 7a). However, in a few areas up to 2% of the cells of the total tumor population had only a thin cytoplasmic rim of GFAP positivity, consistent with the staining pattern of minigemistocytes or gliofibrillary oligodendrocytes (Fig. 7b). In both cases, there was also dense peritumoral reactive astrocytosis, as illustrated by GFAP positivity. There was positive staining of tumor cell nuclei with MIB-1 in as high as 15% and 4% of cells in cat Nos. 1 and 2, respectively (Fig. 8). There was no positive staining on any paraffin-embedded or frozen sections of the tumors with the anti-oligodendroglial antibody nor for galactocerebroside, CD57/HNK-Leu7, MBP, synaptophysin, or triple neurofilament proteins. A few CD45R-positive cells were scattered randomly throughout both tumors.

### Electron microscopy

Tumor cells from cat No. 2 were examined ultrastructurally. The cells had a uniformly round nucleus

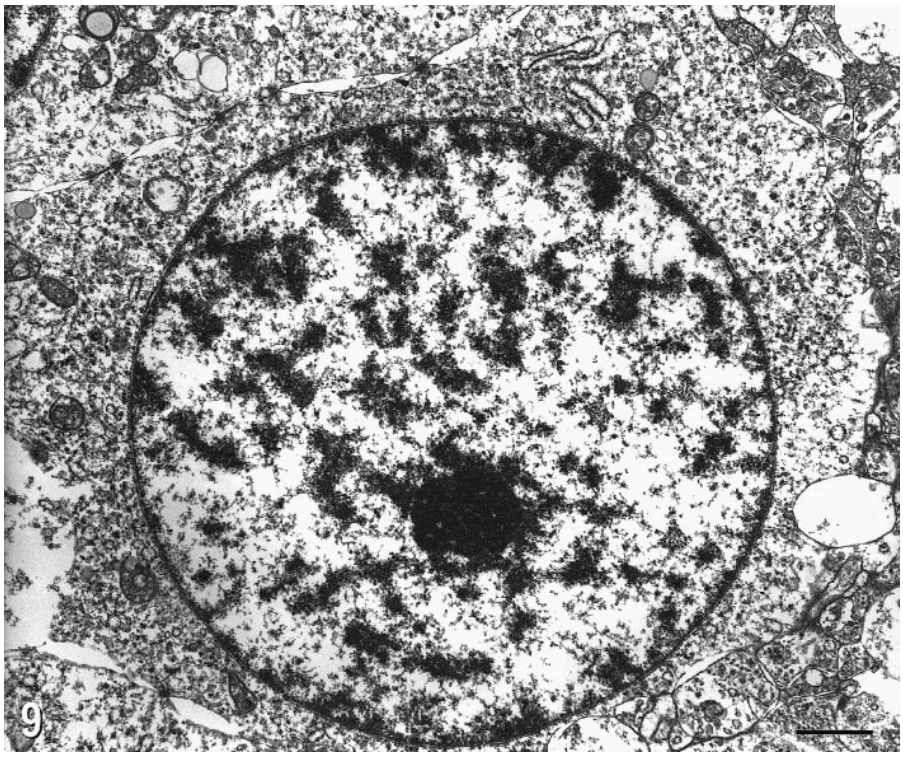

**Fig. 9.** Electron micrograph. Oligodendroglioma, brain; cat No. 2. Note the round nucleus, prominent nucleolus, sparse cytoplasm with few mitochondria and RER. There are numerous intercellular desmosomal and gap junctions. Bar = 0.1 μm.

with a prominent nucleolus and heterochromatin evenly dispersed in clumps. The minimal amount of cytoplasm contained a few profiles of rough and smooth endoplasmic reticulum, abundant free ribosomes, occasional small mitochondria and small vesicles, and very few microtubules. The cytoplasmic membrane was connected to adjacent cells by many short desmosome-like junctions and occasional gap junctions (Fig. 9). There was no evidence of structural myelin formation.

## Discussion

Neuroimaging, clinical neurologic examination, CSF analysis, microscopic and ultrastructural evaluation, and immunocytochemistry were used to evaluate oligodendrogliomas in the brains of two domestic cats. MRI characteristics of both cases were similar with heterogenous contrast enhancement and hyperintensity on PW and T2-weighted images and either iso- or hypointensity on the T1-weighted images. Human oligodendrogliomas exhibit a wide spectrum of features with variable contrast enhancement, sometimes with calcification.[2,13] The calcification in human oligodendrogliomas is more often detected with computed tomography (CT) and may explain the negative findings on the MRI images in the one feline oligodendroglioma with prominent calcification.[13,14] The postcontrast ring enhancement reported in three canine oligodendrogliomas on CT scans was not seen in the MRI scans of these feline tumors.[10,22]

An interesting diagnostic feature of both cases was that presumptive oligodendroglioma cells were identified on the cytospin preparations. However, tumor cells were identified retrospectively following the pathologic diagnosis from necropsy. Although there was an inflammatory CSF profile from analysis of one cat, there was no inflammatory cell response detected microscopically either peri- or intratumorally. Based on our findings, the differential clinical diagnosis of a cat presenting with an inflammatory CSF profile and multifocal brain lesions on MRI must therefore include the unlikely possibility of an oligodendroglioma.

Both cats had large mass lesions distending the fourth ventricle, cerebellum, and midbrain, but it was not possible to determine the site of origin of these tumors. However, in view of these two cases, a similar location in the one well-documented case, and one other report, this area may represent a predilection site for feline oligodendrogliomas.[17,18] However, other cases were reported in the cerebral hemispheres.[12,17] The extensive growth of one tumor into the basilar subarachnoid space with entrapment of multiple cranial nerve roots is a common feature in human oligodendrogliomas.[1,2,14] Histologically, one tumor was classified as an

anaplastic oligodendroglioma with nuclear pleomorphism and hyperchromasia, extensive intratumoral necrosis, very prominent vascularization, and a high mitotic index.[1,2,14] This tumor was also distinctive because of the marked intratumoral calcification. Such calcification is common in human oligodendrogliomas but unusual at least in canine oligodendrogliomas.[1,5,14] This potentially helpful clinical diagnostic feature was not detected with the MRI.

The histologic diagnosis of oligodendroglioma tends to be relatively simple in animals,[5] but human oligodendrogliomas share some gross (intraventricular growth) and histologic (calcification and perinuclear halos) similarities to the recently defined central neurocytoma of neuronal origin.[1,14] However, in these feline cases, both the cytological features (vascular proliferation, myxoid-like cysts, and calcification) and the negative staining for neuron-specific antigens would help to exclude this diagnosis. The minimal CD45R staining in both tumors also rules out the more unlikely possibility of a lymphoma.

Immunocytochemistry of oligodendrogliomas in animals has been rarely reported.[20] In 3/11 canine oligodendrogliomas, positive staining for myelin-associated glycoprotein (MAG) on formalin-fixed, paraffin-embedded tissue was detected, although the tumors were negative for GFAP and MBP.[20] Positive staining of human oligodendrogliomas with MAG is extremely rare.[1,2,14] We did not detect galactocerebroside antigen in the unfixed frozen samples taken from one cat, and there was no positive staining with a wider range of oligodendroglial cell or myelin markers in formalin-fixed, paraffin-embedded tissue. Whether this result is due to lack of antigen expression or from masking due to technical artifacts was not determined. However, positive staining of all these markers was detected in fresh frozen normal feline brain tissue. Of comparative interest was the detection of smooth muscle actin expression in the glomeruloid vascular proliferation, which is so distinctive of anaplastic oligodendrogliomas in dogs. The expression of human von Willebrand factor VIII and smooth muscle actin has been detected in these glomeruloid structures in human glioblastoma multiforme and gliosarcomas[21] and has been attributed to the paracrine production by tumor cells of vascular endothelial growth factor and platelet-derived growth factor respectively.[7] Positive staining for CD57/HNK-leu7, an epitope found in MAG, occurs in up to 90% of human and rat oligodendrogliomas, but this labeling also is found in human astrocytomas and other CNS tumors.[16]

Normal oligodendrocytes do not express GFAP, but immunoreactivity for GFAP can be demonstrated in up to 50% of all human oligodendrogliomas.[2,14] This staining has been attributed in part to classical reactive gemistocytic astrocytes. But a second morphological cell type with positive GFAP immunostaining, the minigemistocyte or gliofibrillary oligodendrocyte (GFOC), may be a transitional form between neoplastic oligodendrocytes and astrocytes.[2,11] On HE staining, this cell appears identical to an oligodendroglioma cell but has a thin perinuclear rim of GFAP-positive cytoplasmic staining.[2] Staining patterns of both cell types were found, but only minigemistocytes or GFOCs were found in cat No. 2. The presence of GFOCs in human oligodendrogliomas neither changes the histologic diagnosis nor modifies the clinical prognosis.[11]

The ultrastructural features of feline oligodendrogliomas have not been described. In the one tumor examined ultrastructurally, the number, type, and distribution of organelles was similar to that described in human oligodendrogliomas; the main differences were the higher density of intercellular desmosomal junctions and a relative paucity of microtubules in the feline oligodendroglioma.[1,2,14]

## Acknowledgement

We acknowledge Steve Maslowski for his superb technical assistance with the MRI studies.

## References

1 Bruner JM: Oligodendroglioma. Semin Diagn Pathol **4:** 251–261, 1988
2 Burger PC, Scheithauer BW: Tumors of neuroglia and choroid plexus epithelium. *In:* Tumors of the Central Nervous System, Atlas of Tumor Pathology, 3rd series, fasc. 10, pp. 107–120. Armed Forces Institute of Pathology, Washington, DC, 1993
3 Cooper ERA, Howarth I: Some pathological changes in the cat brain. J Comp Pathol **66:**35–38, 1956
4 Cusick AJ, Parker PK: Brain stem gliomas in cats. Vet Pathol **12:**460–461, 1975
5 Fankhauser R, Luginbuhl H, McGrath JT: Tumors of the nervous system. Bull World Health Org **50:**53–69, 1974
6 Gafner F, Horning B: Mikrofilarien bei einer Katze. Schweitz Arch Tierheilkd **130:**651–654, 1988
7 Haddad SF, Moore SA, Schelper RL, Goeken JA: Vascular smooth muscle hyperplasia underlies the formation of glomeruloid vascular structures of glioblastoma multiforme. J Neuropathol Exp Neurol **51:**488–492, 1992
8 Hayes HM Jr, Priester WA, Pendergrass TW: Occurrence of nervous-tissue tumors in cattle, horses, cats and dogs. Int J Cancer **15:**39–47, 1975
9 Higgins RJ, LeCouteur RA, Kornegay JN, Coates JR: Late-onset progressive spinocerebellar degeneration in Brittany Spaniel dogs. Acta Neuropathol **96:**97–101, 1998
10 Kraft SL, Gavin PR, DeHaan C, Moore M, Wendling LR, Leathers CW: Retrospective review of 50 cases of canine intracranial tumors evaluated by magnetic resonance imaging. J Vet Intern Med **11:**218–225, 1997
11 Kros JM, Van Eden CG, Stefanko SZ, Waayer-Van Batenburg, van der Kwast TH: Prognostic implications of

glial fibrillary acidic protein containing cell types in oligodendrogliomas. Cancer **66:**1204–1212, 1990
12 LeCouteur RA, Fike JR, Cann CE, Turrel JM, Thompson JE, Biggart JF: X-ray computed tomography of brain tumors in cats. J Am Vet Med Assoc **183:**301–305, 1983
13 Lee C, Duncan VW, Young AB: Magnetic resonance features of the enigmatic oligodendroglioma. Invest Radiol **33:**222–231, 1998
14 McLendon RE, Enterline DS, Tien RD, Thorstad WL, Bruner JM: Tumors of central neuroepithelial origin. *In:* Russell and Rubinstein's Pathology of Tumors of the Nervous System, ed. Bigner DD, McLendon RE, and Bruner JM, 6th ed., pp. 307–572. Oxford University Press, New York, NY, 1998
15 Olivry T, Moore PF, Naydan DK, Danilenko DM: Investigation of epidermotropism in canine mycosis fungoides: expression of intercellular adhesion molecule-1 (ICAM-1) and β-2 integrins. Arch Dermatol Res **288:** 579–585, 1995
16 Perentes E, Rubinstein LJ: Immunohistochemical recognition of human neuroepithelial tumors by anti-Leu7 (HNK-1) monoclonal antibody. Acta Neuropathol **69:** 227–233, 1986
17 Small E: Diseases of the central nervous system. *In:* Feline Medicine and Surgery, ed. Catcott EJ, 1st ed., pp. 303–314. American Veterinary Publications, Santa Barbara, CA, 1964
18 Smith DA, Honhold N: Clinical and pathological features of a cerebellar oligodendroglioma in a cat. J Small Anim Pract **29:**269–274, 1988
19 Summers BA, Cummings JF, de Lahunta A: Tumors of the central nervous system. *In:* Veterinary Neuropathology, pp. 351–401. Mosby, St. Louis, MO, 1995
20 Vandevelde M, Fankhauser R, Luginbuhl H: Immunocytochemical studies in canine neuroectodermal brain tumors. Acta Neuropathol **66:**111–116, 1983
21 Wesseling P, Schlingemann RO, Rietveld FJ, Link M, Burger PC, Ruiter DJ: Early and extensive contribution of pericytes/vascular smooth muscle cells to microvascular proliferation in glioblastoma multiforme: an immuno-light and immuno-electron microscopic study. J Neuropathol Exp Neurol **54:**304–310, 1995
22 Wolf M, Pedroia V, Higgins RJ, Koblik PD, Turrel JM, Owens JM: Intracranial ring enhancing lesions in dogs: a correlative CT scanning and neuropathologic study. Vet Radiol Ultrasound **36:**16–20, 1995
23 Zaki FA, Hurvitz Al: Spontaneous neoplasms of the central nervous system of the cat. J Small Anim Pract **17:** 773-782, 1976

Reprint requests from Dr. R. J. Higgins, Department of Pathology, Microbiology and Immunology, School of Veterinary Medicine, University of California, Davis, CA 95616 (USA). E-mail: rjhiggins@ucdavis.edu.